Annals of R.S.C.B., ISSN:1583-6258, Vol. 27, Issue 1, 2023, Pages. 64-75
.Received 25 December 2022; Accepted 01 January 2023

# Histological Comparison of White Mouse Liver Dosed Experimentally with *Escherichia Coli* O157:H7 and Treated with a Drug and Antibiotic

Ateen Amer Hameed, Prof. Dr. Khulood Naji Rasheed, Prof. Dr. Hala Mohamed Majeed

**Abstract**

The current study is conducted to detect the pathogenicity of *E. coli* O157: H7 and know the effects of its experimental infection in the histological structure of the liver of male mice aged (8-12) weeks. In addition, it attempts to determine the therapeutic effect of an approved drug in the treatment of bacteria and compare it with the antibiotic whose effectiveness is tested *in vitro*. The antibiotic sensitivity test results show that the bacteria are sensitive to Trimethoprim-Sulfamethoxazole, Metronidazole, Gentamicin, Amikacin, Tetracycline, Azithromycin, Ceftriaxone and Ciprofloxacin, and resistant to Amoxicillin/clavulanic acid and Ampicillin. The most sensitive antibiotic is Ciprofloxacin, followed by Trimethoprim-Sulfamethoxazole. Since the latter is an approved and widely used antibiotic, it is chosen with Ciprofloxacin to determine its therapeutic effect against the bacteria under study. Animals experimentally infected with this bacteria show different degrees of clinical signs represented by lethargy, recluse, loss of appetite, increase in respiratory rate and heart beat rate with different degrees of diarrhea appearing in a number of them. In others, different forms of paralysis appear, either paralysis of the hind feet or complete immobilityy, in addition to the occurrence of a number of deaths in mice infected experimentally with the infectious dose of bacteria. As for the results of the histological examination, they are represented in hypertrophy and sometimes hyperplasia in the hepatocytes, loss of chromatin of the nuclei in a number of them with expansion of blood sinusoids, congestion of blood vessels as well as hemorrhage and inflammatory cellular infiltration. These symptoms are more severe in the half lethal dose group (LD-50). As for the groups treated with the two aforementioned antibiotics, it is noted that they play an effective role in stopping diarrhea with mice somewhat regaining their activity. However, they still had suffered from various tissue lesions represented by necrosis, vacuolation, degeneration, inflammatory cellular infiltration, congestion and hemorrhage.

## 1- Introduction

*Escherichia coli* belongs to the Enterobacteriaceae, and is an endemic normal flora of the large intestine in humans and other mammals (Sejal and Leonard, 2015). This harmless bacterium usually becomes a highly adaptive pathogen, capable of causing various diseases in healthy individuals, especially those suffering from immunodeficiency, by obtaining a mixture of mobile genetic elements (Li *et al*., 2019).

Enterohemorrhagic *Escherichia coli* is regarded as the leading cause of outbreaks of diarrheal diseases, hemolytic uremic syndrome (HUS), and hemorrhagic colitis (HC) in

Annals of R.S.C.B., ISSN:1583-6258, Vol. 27, Issue 1, 2023, Pages. 64-75
.Received 25 December 2022; Accepted 01 January 2023

humans and animals (Tse *et al*., 2018). The O157:H7 serotype is a common pathogen between humans and animals, transmitted through food and is responsible for most cases of enterohaemorrhagic diarrhea in humans (Dulo, 2014).

The mechanism followed by this bacteria in causing pathogenicity is not fully understood, but the virulence factors that it possesses have a major role in the occurrence of the disease, the most important of which is the Shiga toxins. The bacteria that produce Shiga toxin are called Shiga Toxin *E. coli* (STEC). It causes damage to the intestinal vascular lining, and this effect has been observed in people with hemorrhagic colitis and hemolytic uremic syndrome (Fatima and Aziz, 2019). It also has the ability to resist the acidic environment, produce the hemolysin enzyme, possesses fimbriae that adhere to the epithelial cells of the urinary system, as well as flagella that make it able to adhere to the cells lining the intestine. In addition, it leads to the formation of adhesion lesions and damage to the intestinal villi, which leads to a decrease in the absorption capacity of the intestinal mucosa and thus an imbalance in the ion balance leading to the occurrence of diarrhea. It is obvious to notice severe tissue damage and lesions in the liver, as it is the organ in which many substances entering the body are metabolized and detoxified in one way or another. Mescher (2016) states that the liver is the organ responsible for detoxification. Through this organ, the body releases the largest possible amount of toxic substances by breaking down the unwanted substance, or through interactions associated with the formation of other compounds that help the body release and excrete it through the kidneys with urine. Approximately (75%) of the blood incoming to the liver comes from the gastrointestinal tracts and the spleen via the portal vein. This blood brings with it the absorbed substances in a concentrated manner, and the liver enzymes work to detoxify some of the substances contained in it (Feng *et al*., 2014).

## 2- Materials and methods

**2.1 chemicals and culture agars:** the traditional MacConkey agar is used to isolate the bacteria. The SMAC agar is used to confirm its diagnosis, while the HiCrome agar is regarded as one of the selective media for *E.coli* O157:H7 as EMB agar. The chemicals formalin, ethanol, xylene, paraffin, Hematoxylin, Eosin, and D.P.X are used in the preparation of histological sections of the liver.

### 2.2 Bacterium Isolate

The diagnosed and ready-to-use *E.coli* O157:H7 isolate is used. Despite this, some culture laboratory tests are performed to confirm the validity of its diagnosis. Its type is also determined by biochemical tests using the VITEK® 2 Compact device. The Antibiotic susceptibility testing is carried out using the modified Bauer-Kirby method (Bauer *et al.*, 1966) approved by the World Health Organization.

Annals of R.S.C.B., ISSN:1583-6258, Vol. 27, Issue 1, 2023, Pages. 64-75
.Received 25 December 2022; Accepted 01 January 2023

### 2.3 Determination of the half lethal dose (LD-50), the infectious dose, and the bacterial count

The half lethal dose and the infectious dose are determined according to the Reed-Muench method (1938). As for the bacterial count, the Pour plate method is used for its determination.

### 2.4 The Experimental Design

Forty-eight male mice of the Balb/c strain, aged (8-12) weeks, weighing between (22-28) gm, are used. They are randomly distributed into six groups of (8) mice per group, as follows:

1- The first group (the control group): a group of mice treated with a physiological solution at a rate of 1 ml for one time per day.
2- The second group: a group of mice treated with the half lethal dose (LD-50) of *E.coli* O157:H7 at a concentration of $9\times10^2$ cell/ml.
3- The third group: a group of mice treated with the infectious dose of bacteria at a concentration of $5\times10^5$ cell/ml.
4- The fourth group: thae group of mice treated with the antibiotic Trimethoprim-Sulfamethoxazole by1 ml per day at a concentration of 102.88 mg / kg according to Nair and Jacob (2016).
5- The fifth group: a group of mice treated with the antibiotic Ciprofloxacin by 1 ml at a concentration of 102.88 mg / kg according to Nair and Jacob (2016).
6- The sixth group: a group of mice treated with the two antibiotics Trimethoprim-Sulfamethoxazole and Ciprofloxacin together at a concentration of 102.88 mg/kg each.

After that, glass slides are made using the section method of the liver tissue by adopting the Luna (1968) method, which includes: fixation, washing, dehydration, clearing, infiltration , embedding, trimming and sectioning, staining, and mounting. Finally, the tissue glass slides are examined and photographed under a light microscope at different magnification powers.

## 3- Results and Discussion

### 3.1 Confirming the diagnosis of *E.coli* O157:H7

The diagnosis of the bacteria under study with its type is confirmed based on bacterial isolation on traditional and selective culture media agars, and biochemical tests using the Vitek device as illustrated in Figures (3-1), (3-2), (3-3), (3-3), (3-4) and Table (3-1).

Annals of R.S.C.B., ISSN:1583-6258, Vol. 27, Issue 1, 2023, Pages. 64-75
.Received 25 December 2022; Accepted 01 January 2023

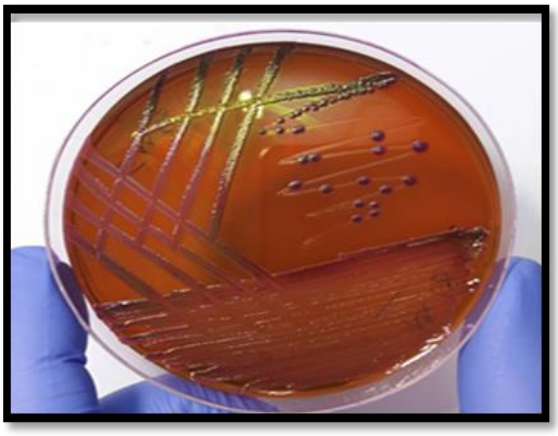

**Figure (3-2): *E.coli* on EMB agar**

**Figure (3-1): *E.coli* on MacConkey agar**

**Figure (3-4): *E.coli* O157:H on SMAC agar**

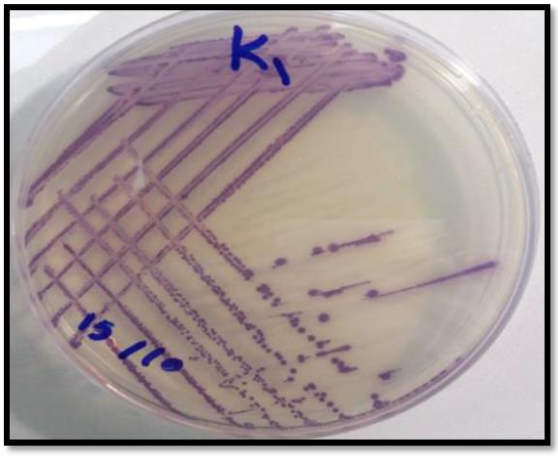

**Figure (3-3):*E.coli* O157:H7 on HiCrome agar**

**Table (3-1): Biochemical diagnosis using the Vitek device**

| | | | | | |
|---|---|---|---|---|---|
| **Identification Information** | **Card:** GN | **Lot Number:** 2411419403 | **Expires:** Oct 15, 2021 13:00 CDT |
| | **Status:** Final | **Analysis Time:** 10.00 hours | **Completed:** Apr 2, 2021 12:23 CDT |
| **Organism Origin** | VITEK 2 | | |
| **Selected Organism** | 98% Probability **Escherichia coli O157**<br>Bionumber: 0405611140567251 Confidence: Excellent identification | | |
| **Analysis Organisms and Tests to Separate:** | | | |
| **Analysis Messages:**<br>Confirm by serological tests<br>Highly pathogenic organism | | | |
| **Contraindicating Typical Biopattern(s)**<br>Escherichia coli O157 SAC(80), | | | |

| **Biochemical Details** | | | | | | | | | | | | | | | | | |
|---|---|---|---|---|---|---|---|---|---|---|---|---|---|---|---|---|---|
| 2 | APPA | - | 3 | ADO | - | 4 | PyrA | - | 5 | lARL | - | 7 | dCEL | - | 9 | BGAL | + |
| 10 | H2S | - | 11 | BNAG | - | 12 | AGLTp | - | 13 | dGLU | + | 14 | GGT | - | 15 | OFF | + |
| 17 | BGLU | - | 18 | dMAL | + | 19 | dMAN | + | 20 | dMNE | + | 21 | BXYL | - | 22 | BAlap | - |
| 23 | ProA | + | 26 | LIP | - | 27 | PLE | - | 29 | TyrA | + | 31 | URE | - | 32 | dSOR | - |
| 33 | SAC | - | 34 | dTAG | - | 35 | dTRE | + | 36 | CIT | - | 37 | MNT | - | 39 | 5KG | - |
| 40 | lLATk | + | 41 | AGLU | - | 42 | SUCT | + | 43 | NAGA | - | 44 | AGAL | + | 45 | PHOS | + |
| 46 | GlyA | + | 47 | ODC | + | 48 | LDC | + | 53 | lHISa | - | 56 | CMT | + | 57 | BGUR | - |
| 58 | O129R | + | 59 | GGAA | - | 61 | lMLTa | + | 62 | ELLM | + | 64 | lLATa | - | | | |

Our results agree with Al-Taie (2020) in his study of isolating and diagnosing *E.coli* O157:H7. They appear as pink colonies on the MacConkey agar since they ferment lactose sugar, while characterized by the phenomenon of metallic luster on EMB agar. Our results

Annals of R.S.C.B., ISSN:1583-6258, Vol. 27, Issue 1, 2023, Pages. 64-75
.Received 25 December 2022; Accepted 01 January 2023

also agree with Yadav *et.al* (2018) in the appearance of typical colonies of these colorless bacteria as they do not ferment the sorbitol sugar on SMAC agar, while the pink-purple colonies indicate *E.coli* O157:H7. In a study conducted by Klaif *et. al* (2019), they have found that the HiCrome agar of *Escherichia coli* bacteria of the O157:H7 serotype is useful for the diagnosis of this bacteria.

### 3.2 Testing the sensitivity of *E.coli* O157:H7 to antibiotics

A sensitivity test is conducted towards (10) types of different antibiotics. The results show that the bacteria are sensitive to the antibiotics Trimethoprim-Sulfamethoxazole, Metronidazole, Gentamicin Amikacin, Azithromycin, Ceftriaxone, Ciprofloxacin and Tetracycline, and are resistant to Amoxicillin/clavulanic acid and Ampicillin. It is to be noted that the bacteria are more sensitive to the antibiotic Ciprofloxacin, followed by the antibiotic Trimethoprim-Sulfamethoxazole, as shown in Figures (3-5) and (3-6).

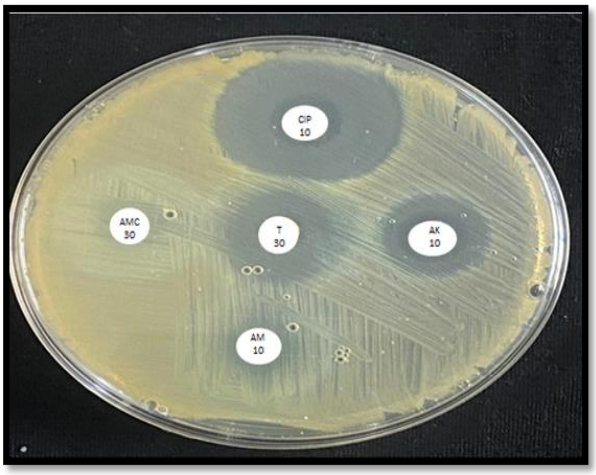


**Figure (3-6): Bacterial sensitivity to Amikacin, Tetracycline and Ciprofloxacin and their resistance to Amoxicillin/clavulanic acid and Ampicillin**

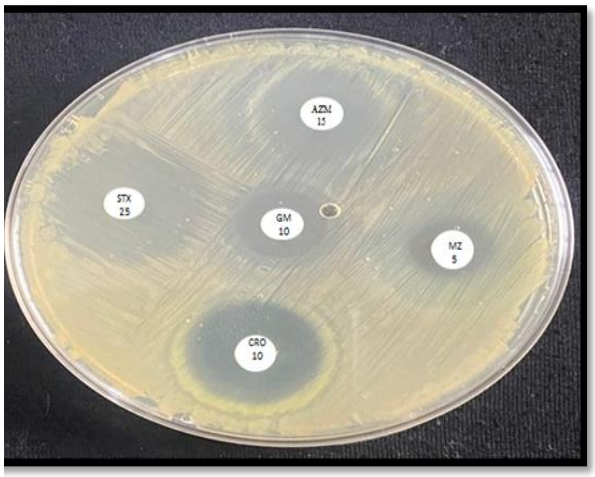


**Figure (3-5): Bacterial sensitivity to the antibiotics Trimethoprim-Sulfamethoxazole,Metronidazole, Gentamicin, Azithromycin and Ceftriaxone**

Our results agree with what is reached by Tawfiq (2006) in his study on coliform bacteria isolated in hospitals in Saudi Arabia in that their resistance to ampicillin was high. The results by Ali (2012) supported this, with the exception of the results regarding the resistance of the bacteria to the antibiotics Trimethoprim and Amoxicillin/ clavulanic acid in which our results do not agree with his. Also, our results do not agree with Nguyen et. al.(2005) who reached the same result. As for our results regarding the sensitivity of *E.coli* to Ciprofloxacin and Trimethoprim, they agree with the results of Mahdi (2019).

### 3.3 The Histological Examination

The histopathological examination of the first group of mice shows the normal structure of the visceral tissue of the liver, which is composed of hepatic cords or sheets formed by

polygonal hepatic epithelial cells. The distinctive shape of the hepatocytes is radially arranged around the central vein, separated by bloody spaces representing sinusoids containing phagocytic Kupffer cells, as in Figure (3-7). As for the second group, the results reveal pathological changes represented by acute necrosis in a number of hepatocytes, vacuolation of their cytoplasm, loss of its chromatin material and thickening of the nuclei of a number of others. In addition, there is congestion of the central vein and inflammatory cellular infiltration around it with an increase in the number and size of Kupffer cells as in Figures (3-8) and (3-9). Changes are also observed in the portal triad, represented by severe hyperemia in the branch of the portal vein, with thickening and fibrosis of its walls, hemolysis in the branch of the hepatic artery, and hyperplasia of the lining of the bile duct, as shown in Figure (3-10). The histological sections of the third group show acute necrosis of the hepatocytes, thickening of the nuclei, vacuolation of parts of the tissue, cellular debris, with inflammatory cellular infiltration, as well as an increase in the number of Kupffer cells. Moreover, there is severe damage to the wall of the central vein which leads to severe hemorrhage and the formation of an inflammatory exudate containing red blood cells, as shown in Figures (3-11) and (3-12). The histological changes of the fourth group are represented by vacuolar degeneration of a number of hepatocytes and necrosis of others, vacuolation of the cytoplasm, hypertrophy in some Kupffer cells. There is also diffuse congestion in the sinusoids, the central vein and the branch of the portal vein, with inflammatory cellular infiltration around the blood vessels and the bile cannula branch as in Figures (3-13), (3-14), (3-15).

The results of the fifth group also indicate necrosis in a number of hepatocytes, with hypertrophy of Kupffer cells, cellular infiltration around the two branches of the hepatic artery, the bile duct, and the two branches of the lymphatic vessel. In addition, there is the occurrence of thrombosis in the hepatic portal vein branch, hemolysis in the central vein with partial damage in its wall, and the presence of diffuse bleeding as in Figures (3-16), (3-17), (3-18). As for the sixth group, the results show the persistence of pathological changes after treatment with both antibiotics and the absence of signs of improvement in mice. This is represented by necrosis, vacuolation, loss of chromatin material for a number of nuclei, thickening of the nuclear membrane of a number of nuclei, hypertrophy in a number of hepatocytes, increase in the number and size of Kupffer cells, expansion of the blood sinusoids and their congestion with blood, and the presence of a thrombus in the central vein. As shown in Figures (3-19), (3-20), (3-21).

Annals of R.S.C.B., ISSN:1583-6258, Vol. 27, Issue 1, 2023, Pages. 64-75
.Received 25 December 2022; Accepted 01 January 2023

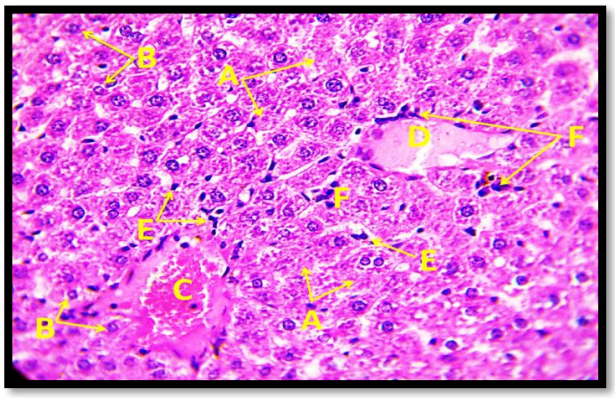


**Figure (3-8): A microscopic image of a section in the liver of a mouse from the second group, in which necrosis is observed in a number of hepatocytes (A), loss of chromatin in the nuclei of a number of others (B), congestion and hemolysis in a central vein (C), hemolysis in another central vein (D), hyperplasia and hypertrophy of Kupffer cells in blood sinusoids (E) inflammation cells infiltration around and near a central vein (F). (H&E, X40).**

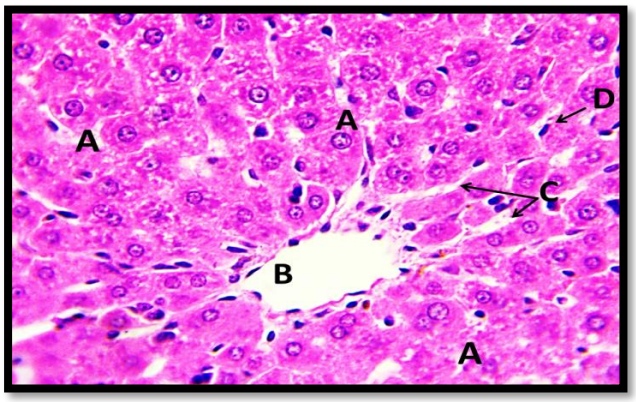


**Figure (3-7): A microscopic image of a section in the liver of a mouse from the first group, in which hepatocytes are arranged radially (A) around the central vein (B) separated by sinusoids (C) containing Kupffer cells (D). (H&E, X40).**

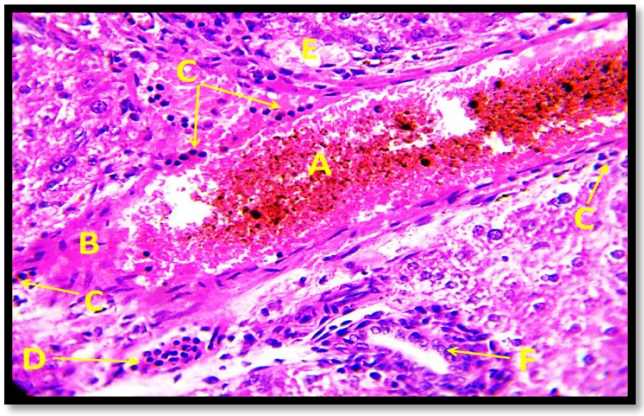


**Figure (3-10): A microscopic image of a section in the liver of a mouse from the second group, in which severe hyperemia is observed in the portal venule branch (A), thickness and fibrosis of its walls (B), infiltration of inflammatory cells around it (C), focal infiltration near it (D), hemolysis in the branch of the hepatic artery (E), hyperplasia of the bile ductule (F). (H&E, X40).**

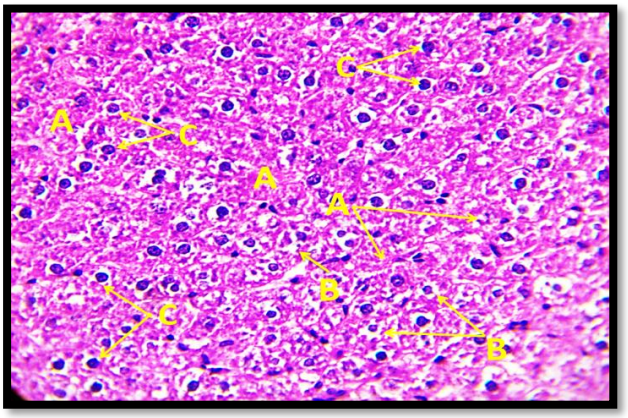


**Figure (3-9): A microscopic image of a section in the liver of a mouse from the second group, in which the observance of necrosis of a number of hepatocytes (A) vacuolation of the cytoplasm of a number of others (B), and pyknosis of the nuclei throughout the histological section (C). (H&E, X40).**

Annals of R.S.C.B., ISSN:1583-6258, Vol. 27, Issue 1, 2023, Pages. 64-75
.Received 25 December 2022; Accepted 01 January 2023

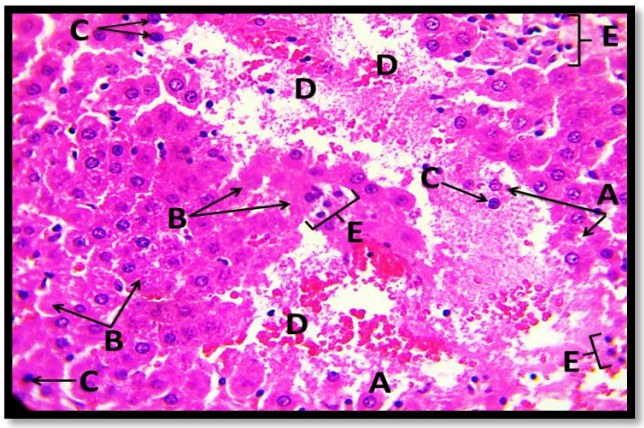


**Figure (3-12): A microscopic image of a section in the liver of a mouse from the third group, in which degeneration (A) and necrosis of a number of hepatocytes (B) are noted, pyknosis of the nuclei in others (C), and severe hemorrhage (D), inflammatory cytokine infiltration (E). (H&E, X40).**

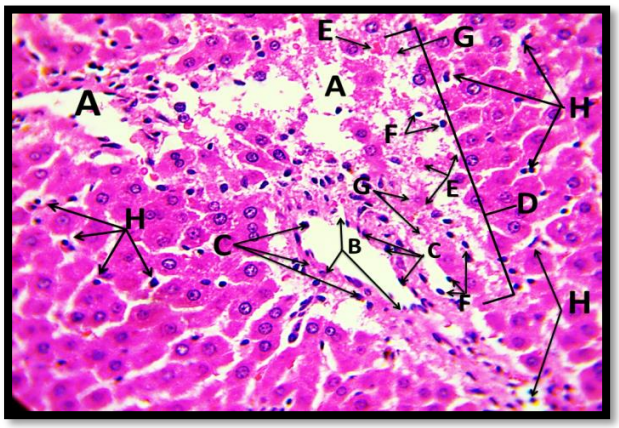


**Figure (3-11): A microscopic image of a section in the liver of a mouse from the third group, in which acute necrosis of the hepatocytes is noted leading to the vacuolation of parts of the tissue (A), severe damage to the wall of the central vein (B), the infiltration of inflammatory cells around it ( C), inflammatory exudate (D) containing erythrocytes (E), lymphocytic infiltration (F), debris (G), increase in number and size of Kupffer cells (H). (H&E, X40).**

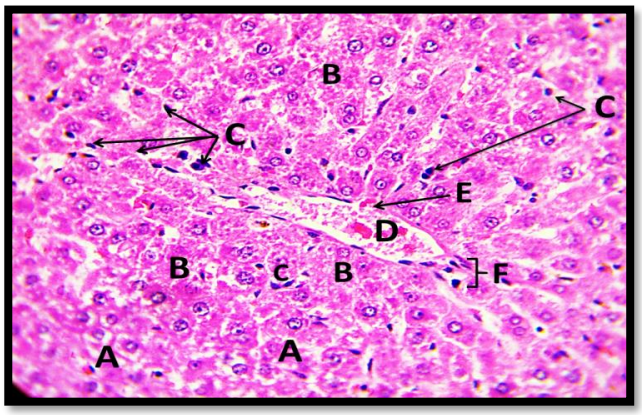


**Figure (3-14): A microscopic image of a section of the liver of a mouse from the fourth group, in which degeneration is observed in a number of hepatocytes with vacuolation of the cytoplasm (A), acute necrosis in a number of others (B), hypertrophy in a number of Kupffer cells ( C), hyperemia of the central vein (D) partial damage to its wall (E) and near inflammatory cellular infiltration (F). (H&E, X40).**

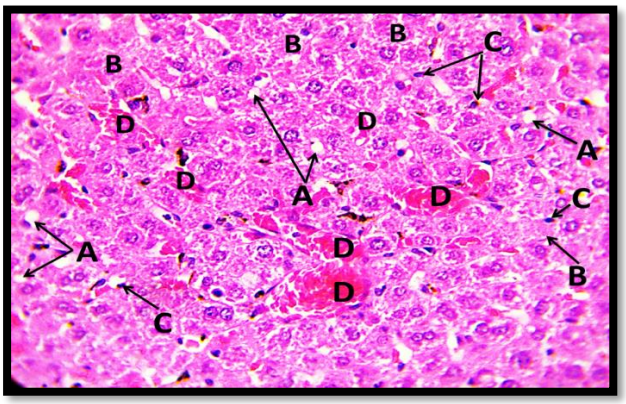


**Figure (3-13): A microscopic image of a section in the liver of a mouse from the fourth group, in which vacuolar degeneration is observed in a number of hepatocytes (A), necrosis in a number of others (B), hypertrophy in some Kupffer cells (C), diffused blood congestion in sinusoids (D). (H&E, X40).**

Annals of R.S.C.B., ISSN:1583-6258, Vol. 27, Issue 1, 2023, Pages. 64-75
.Received 25 December 2022; Accepted 01 January 2023

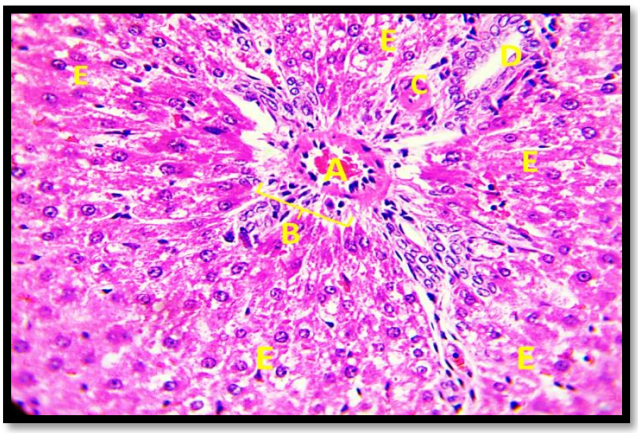


**Figure (3-16): Microscopic image of a section of the liver of a fifth group mouse, in which thrombus is observed in the portal vein branch (A) with inflammatory cellular infiltration around it (B) and around each of the hepatic artery branch (C) and the bile duct branch (D), vacuolation in the cytoplasm of most hepatocytes (E). (H&E, X40).**

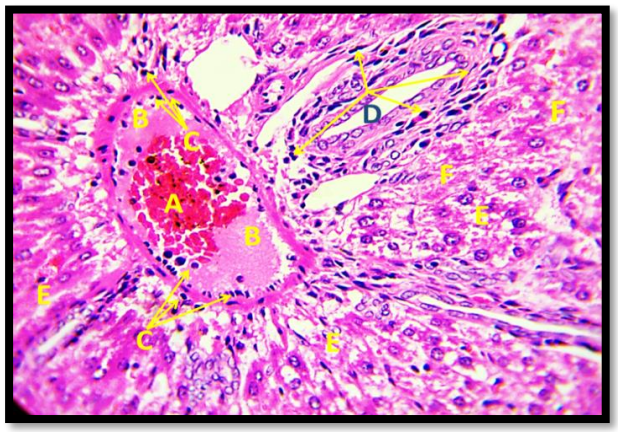


**Figure (3-15): Microscopic image of a section of the liver of a mouse from the fourth group, in which congestion (A) and hemolysis are observed in the portal vein branch (B) with infiltration of inflammatory cells at its periphery (C), in addition to their infiltration around the bile duct branch ( D), degeneration (E) and necrosis of hepatocytes (F). (H&E, X40).**

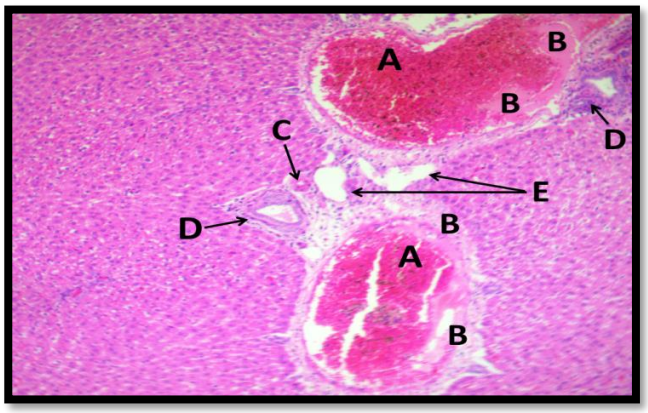


**Figure (3-18): Microscopic image of a section in the liver of a mouse from the fifth group, in which acute blood congestion is observed in the two branches of the portal vein (A) partial hemolysis in them (B), inflammatory cellular infiltration around each of the branches of the hepatic artery (C). Two ductal bile branches (D) and two lymphatic vessels (E). (H&E, X4).**

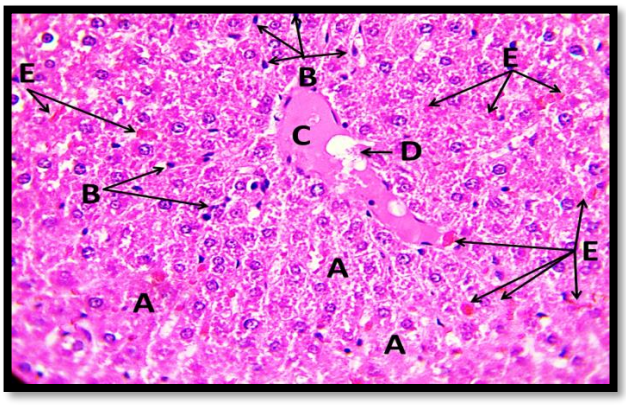


**Figure (3-17): A microscopic image of a section of the liver of a mouse from the fifth group, in which necrosis is observed in a number of hepatocytes (A), hypertrophy in some Kupffer cells (B), hemolysis in the central vein (C) partial damage In its wall (D), hemorrhage spread throughout the histological section (E). (H&E, X40).**

Annals of R.S.C.B., ISSN:1583-6258, Vol. 27, Issue 1, 2023, Pages. 64-75
.Received 25 December 2022; Accepted 01 January 2023

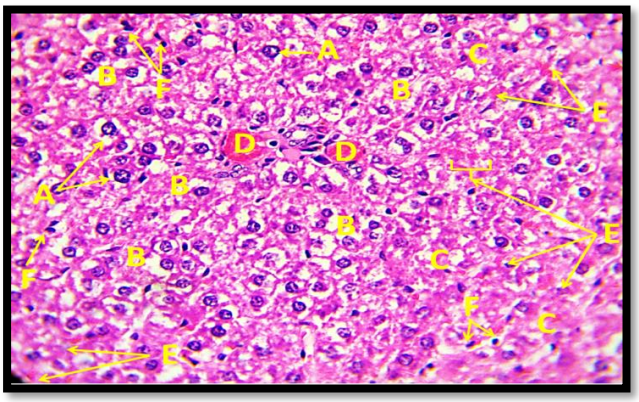


**Figure (3-20): A microscopic image of a section in the liver of a mouse from the sixth group, in which an hypertrophy of some hepatocytes (A), a general vacuolation in the cytoplasm of cells (B), necrosis in a number of others (C), two dilated Sinusoids and their blood congested (D), hemorrhage spread throughout the histological section (E), Kupffer cell hypertrophy (F). (H&E, X40).**

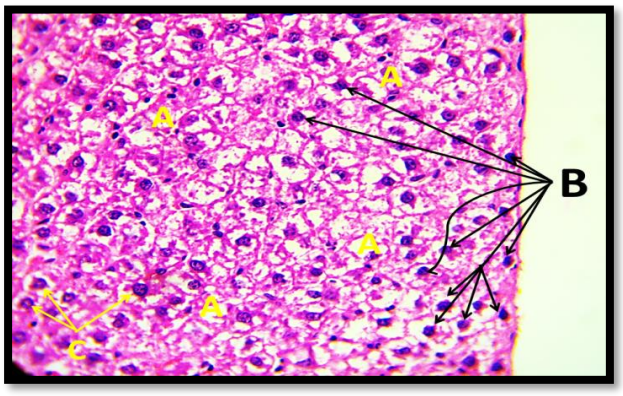


**Figure (3-19): A microscopic image of a section in the liver of a mouse from the sixth group, in which the cytoplasm of hepatocytes vacuolates throughout the histological section (A), nuclei pyknosis of a number of cells (B), and the nuclear envelope thickens in a number of others (C). (H&E, X40).**

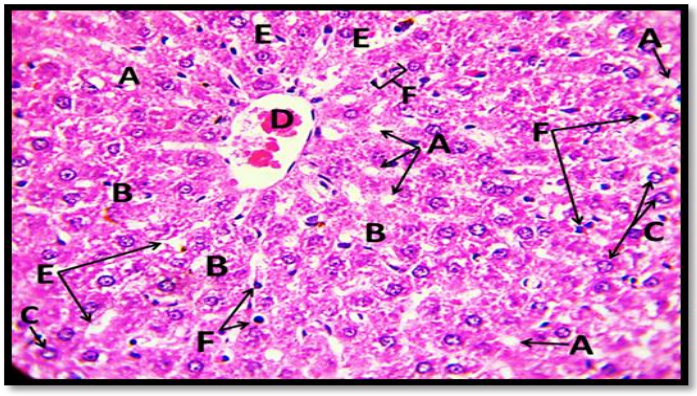


**Figure (3-21): Microscopic image of a section in the liver of a mouse from the sixth group, in which vacuolar degeneration is observed in a number of hepatocytes (A), necrosis in a number of others (B), loss of chromatin in a number of nuclei (C), central venous thrombosis (D), dilatation of some sinusoids (E), increased number and size of Kupffer cells (F). (H&E, X40).**

The occurrence of histological lesions is attributed to the action of endotoxins that are part of the components of the wall of Gram-negative bacteria. the arrival of *E.coli* O157:H7 to the liver tissue leads to the occurrence of an inflammatory defense response by the tissue (Rubin and Reisner, 2009). The cause of the gathering of defensive cells is due to the decomposition of the hepatocytes, which leads to the liberation of substances that have the ability to chemically attract the devoured defensive cells in order to get rid of them, which in

turn causes the death and decomposition of more cells. This is consistent with what Mahdi (2019) has reported in that damaged hepatocytes release compounds such as prostaglandin E1 that have the ability to chemically attract the neutrophils. He has also indicated that neutrophils migrate to the inflamed tissue and secrete a chemo-attractant to attract more of them. In addition, the proteins released as a result of cell damage are subject to partial degradation, which leads to making the proteins chemically attractive to the defensive cells. Moreover, damage to the walls of blood vessels leads to hemorrhage and proliferation of red blood cells in the parenchyma of the liver tissue (Kumar, 2016).

The occurrence of congestion in the blood vessels of the liver tissue is attributed to the local reduction of venous blood flow as a result of occlusion in the blood vessels supplying the part in which the congestion has occurred. This may be due to the presence of large amounts of lipopolysaccharide, which leads to impairment of liver function by damaging the hepatic vascular tissue, and may lead to blockage of blood vessels and thus a decrease in the amount of blood supplied to the tissue and then tissue death (AL-Jobory *et al*., 2018). The infiltration of lymphocytes in the liver tissue is one of the tissue's defenses against the causative agent. As for the increase in the number of Kupffer cells, it is only a result of inflammation of the liver tissue due to bacteria or their toxins. Our results agree with what has been found by Khalifa *et al.* (2005), who indicate that *E.coli* O157:H7 causes severe histopathological lesions in the liver due to the direct effects of the bacteria and their toxins on hepatocytes. It also agrees with the findings of Chabek (2010), who obtained the same results when administering mice with *E.coli* O157:H7. These results state that the pathological changes are represented by the presence of degenerative changes resulting from the fact that the germ has the ability to produce some substances that cause tissue changes. For example, the possession of this bacteria of lipopolysaccharides, which is characterized by its direct action on the tissues of the host or its effect on the immune system and the liberation of inflammatory mediators, as well as the possession of virulence factors, the most important of which are Shiga toxins that work synergistically in causing histological changes that result from the inflammatory response of the tissue against the causative agent. Polysaccharides induce genes encoding Hypoxia Inducible Factor (HIF-1), which negatively affects tissue (Peyssonaunx *et al.*, 2007).

**References**

[1] **AL-Jobory, M. B.; AL-Thwaini, A. N. and Najeeb, L. M. (2018).** Using sesame oil to treat the infection of hemorrhagic *E.coli* O157:H7 bacteria isolation in Baghdad: Molecular and histological study. *Plant Arch.,* 1(18): 627-637.

[2] **Chabek, S. I. A. (2010).** A study of some virulence factors of the intestinal pathogenic *Escherichia coli* bacteria isolated from acute diarrhea cases in infants in Babylon province. Msc Thesis/ College of Science- University of Babylon.

[3] **Dulo, F. (2014).** Prevalence and antimicrobial resistance profile of *Escherichia coli* O157:H7 in goat slaughtered in dire dawa municipal abattoir as well as food safety knowledge, attitude and hygiene practice assessment among slaughter staff, Ethiopia. MSc, Thesis, Addis Ababa University.

[4] **Fatima, R. and Aziz, M. (2019).** Enterohemorrhagic *Escherichia coli* (EHEC). StatPearls; StatPearls Publishing: Treasure Island, FL, USA.

[5] **Feng, P.; Weagant, S. D. and Jinneman, K. (2014).** Prevalence and diversity of enterotoxigenic *Escherichia coli* strains in fresh produce. *J. Food Prot.*, 77(5): 820-823.

[6] **Khalifa, S. A.; Al-Aliani, R. A. and Al-Alwani, A. D. (2005).** Histological, cellular and histochemical studies of the effect of camel urine on the liver of rabbits infected with *Escherichia coli*. *Saudi J. Biol. Sci.*, 12(2): pp.66-80.

[7] **Klaif, S. F.; Saleh, Z. F.; Hussein, M. T.; Jawad, A. A. and Jawad, M. S. (2019).** Molecular characterization of enterohemorrhagic *E. coli* O157 and O153 isolated from tissue camel and human stool samples in Al-Diwaniyah, Iraq. *Iraqi J. Vet. Sci.*, 33(1): 81-86.

[8] **Kumar, C. R. (2016).** Basic Pathology. 7th ed., Saunders, Philadelphia. London, Toronoto Monteral Sydney Tokyo. 16-33.

[9] **Li, X.; Zhang, Z.; Chang, X.; Wang, X.; Hu, J.; Lin, Q. and Wang, X. (2019).** Disruption of blood-brain barrier by an *Escherichia coli* isolated from canine septicemia and meningoencephalitis. *Comp. Microbiol. Infect. Dis.*, (63): 44-50.

[10] **Luna, L. (1968).** Manual of histological staining methods of the Armed Forces Institute of Pathology. 3rd ed., The Blakiston Division. McGraw- Hill Book Co. New York. U.S.A.

[11] **Mahdi, E. M. (2019).** Histological comparison of the effect of the antibiotic ciprofloxacin and the aqueous and alcoholic extracts of Petroselinum crispu (Minaria) on a number of internal organs of albino mice experimentally infected with *E.coli*. Master Thesis/ College of Science- University of Tikrit.

[12] **Mescher, A. L. (2016).** Junqueira's basic histology: text and atlas 14th ed., McGraw- Hill Education.

[13] **Nair, A. B. and Jacob, S. (2016).** Asimple practice guide for dose conversion between animals and human. *J. Basic clin. Pharm*., (7): 27-31.

[14] **Nguyen, T.; Le Van, P.; Huy Le, C. H . and Weintraub, A. (2005).** Antibiotic Resistance in Diarrheagenic *Escherichia. Vietnam Antimicrob. Agents Chemother.*, 49(2): 816-819.

[15] **Obrig, T. G. (2010).** *Escherichia coli* Shiga toxin mechanisms of action in renal disease. *Toxins*, 2(12): 2769-2794.

[16] **Peyssonuanx, C.; Martin, P. C.; Deendens, A.; Zinkernagel, A. S and Nizer, V. (2007).** Essential role of hypoxia inducible factor 1 in development of lipopolysaccharide induced sepsis. *Immunnity*, (178): 7516-17519.

[17] **Reed, L. J. and Muench, H. (1938).** A simple method of estimating fifty percent end point. *A. J. Hyg.*, 27(3): 493-497

[18] **Rubin, E. and Reisner, H. M. (2009).** Essentials of Rubins Pathology . 2nd ed., Lippincott William & Wilkins. 2-162.

[19] **Sejal, M. and Leonard, R. K. (2015).** *Escherichia coli* Infections. *Ped. Rev.*, 36(4): 4-176.

[20] **Tawfiq, J. A. (2006).** Increasing antibiotic resistance among isolates of *Escherichia coli* recovered from inpatients and outpatients in a Saudi Arabian hospital. *Infect. Control Hosp. Epidemiol.*, 27(7): 748-753.

[21] **Tse, C.; Yin, J.; Donowitz, M.; Doucet, M.; Foulke-Abel, J. and Kovbasnjuk, O. (2018).** Enterohemorrhagic *E. coli* (EHEC) Secreted Serine Protease EspP Stimulates Electrogenic Ion Transport in Human Colonoid Monolayers. *Toxins*, 10(9): 351.

[22] **Yadav, M.; Bhatiani, A.; Bhagoliwal, A.; Kumar, A. and Sujatha, R. (2018).** *Esherichia coli* O157: H7 Serotypes Isolation from Children in Stool Samples. *J. Pure. Appl. Microbiol.*, 12(1): 55-58.